A HIGH-RESOLUTION STUDY OF MERIDIONAL FLOWS NEAR THE SOLAR EQUATOR

Richard S. Bogart[1], **Sarbani Basu**[2], **and Deborah A. Haber**[3]

[1]*CSSA-HEPL, Stanford University, Stanford, CA 94305-4085, USA*
[2]*Astronomy Department, Yale University, PO Box 208101, New Haven, CT 06520-8101, USA*
[3]*JILA, University of Colorado, Campus Box 440, Boulder, CO 80309, USA*

ABSTRACT

From 25 May to 7 June 2004, long uninterrupted observations from MDI were available as SOHO crossed the solar equator. Continuous Doppler data were obtained in a sub-region of the MDI high-resolution field approximately centered in latitude on the equator and spanning the longitudinal width of the field. After the first day of the observing campaign the whole region was magnetically quiet. This dataset provides a unique opportunity to study the dynamical structures near the solar equator at high resolution with differential geometric foreshortening in the two hemispheres effectively removed. We report here on the results of our initial ring-diagram analysis of the data.

1. INTRODUCTION

Data from the MDI high-resolution field allow local ring-diagram analysis to probe the structure and dynamics very near the photosphere by making use of low-order modes extending to high spatial wavenumber. At this resolution the three lowest order sets of modes typically extend to an equivalent spherical harmonic degree (kR_0)of over 1400 (Fig. 1). The opportunities for such analysis have however been limited by the small number of time windows in which sufficiently long runs of continuous high-resolution Doppler data have been available and by the small extent and fixed location of the high-resolution field. The accompanying table lists all MDI campaigns to date for which continuous high-resolution Doppler data have been available for intervals exceeding about 3 days, the time for a solar location to rotate through the field of view. Data from only about half of the field can be fit into the MDI telemetry stream during these campaigns, and the camera field was truncated in the north-south direction, so the effective latitudinal extent of the observed region is about $17^\circ.5$ heliographic.

This year's high-resolution Doppler campaign was the first in which SOHO crossed the solar equatorial plane,

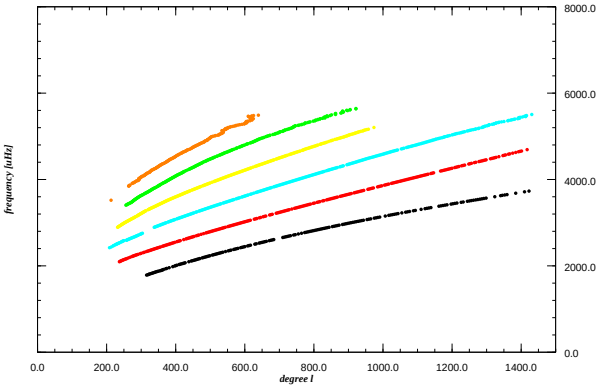

Figure 1. A sample mode set showing the dispersion relation for a single power spectrum. The particular set shown is for the region centered at the equator and at Carrington longitude 2017:340. Modes are color-coded by their radial order, black corrresponding to the $f-$mode.

Table 1. 1. MDI high-res campaigns of duration $> 3d$.

Dates	Field	B_0 Range
1997 June 13–19	1024×640	$[+0^\circ.8, +1^\circ.5]$
1997 June 30 – July 14	1024×640	$[+2.8, +4.3]$
1998 Mar. 7 – Apr. 10	1024×600	$[-7.2, -6.0]$
2001 May 14–28	1024×600	$[-2.8, -1.1]$
2002 May 24 – June 3	1024×600	$[-1.6, -0.4]$
2003 Jan. 18 – Feb. 16	1024×600	$[-6.8, -4.8]$
2004 May 26 – June 7	1024×500	$[-1.3, +0.1]$

Table 2. 2. Duty cycles for selected regions.

Carr Lon	Begin	End	Coverage
2016:025	05/25 15:51	05/28 12:06	0.87
2016:015	05/26 09:58	05/29 06:13	0.85
2016:000	05/27 13:10	05/30 09:25	0.80
2017:340	05/29 01:26	05/31 21:41	0.92
2017:315	05/30 22:45	06/02 19:00	0.78
2017:295	06/01 15:08	06/04 05:50	0.89
2017:285	06/02 05:10	06/05 01:23	0.92
2017:270	06/03 08:19	06/06 00:30	0.86
2017:255	06/04 11:30	06/07 04:30	0.85
2017:245	06/05 05:38	06/08 00:43	0.82

though it was close during the campaign of 2002. However, the magnetic activity was lower and much more uniform this year. During the course of the campaign the latitudinal extent of the observed field went from $[-12°.5, 5°.0]$ to $[-10°.5, 7°.0]$.

2. DATA ANALYSIS

For the ring-diagram analysis we selected 30 regions of diameter $10°$ centered at latitudes $0°$ and $\pm 5°$ and at the ten Carrington longitudes listed in Table 2. The target longitudes were selected to maximize coverage during the tracking intervals of 4096 minutes, the observing duty cycle having been quite variable during the campaign. (In previous campaigns duty cycles usually exceeded 0.95.) Since the observed field did not extend northward of $+7°$, it should be noted that the regions centered at latitude $+5°$ are really only effectively the northern halves of the corresponding regions centered at the equator.

The ten sets of power spectra at different longitudes for each of the three target latitudes were averaged together to produce mean spectra that were then fit and inverted for the meridional velocity parameter by two different techniques. Method 1 uses the fitting procedure described in Basu & Antia (1999), while Method 2 uses the fitting procedure of Haber *et al.*, (2002). Both mode sets were independently inverted for the meridional and zonal advective velocity terms U_y and U_x with OLA inversions.

The high-resolution campaigns of 2001 and July 1997 had been previously tracked. During both of these campaigns it was the northern rather than the southern part of the high-resolution field that had been extracted for telemetry. Conseuquently the areas analyzed in both campaign were well north of the equator, despite the fact that during the 2001 campaign disc center was in the southern hemisphere. Data from these earlier campaigns have been analyzed using the same methods for the sake of comparison.

3. RESULTS

The inferred meridional flows as a function of depth are shown in Fig. 2 and 3 for each of the latitudes analyzed in both the campaign of 2004 and the two comparison campaigns. The zonal flows are shown in Fig. 4 and 5.

As expected from the degree of overlap of the fields, the near-surface flow at $5°$N is generally closer to that at the equator than the flow at $5°$S. At greater depths, the equatorial flow more closely follows the trend at $5°$S. This behaviour is seen in both analyses, though the values of the meridional flow and the depth of the crossover differ. Method 1 shows a symmetric near-surface 10 m/s poleward flow, but with the boundary between the cells evidently a few degrees south of the equator. Method 2 shows similar latititudinal variations, but with a consistent 10 m/s offset, so that the cross-equatorial flow seems to vanish, but with a $\sim$ 20 m/s flow on the south side of the equator. This unexplained discrepancy also seems to exist for the data of the previous campaigns as well.

At greater depths the meridional flows measured on both sides of the equator merge to a common value of about ~ -10 m/s. The merging takes place at a depth of about 10 Mm, whereas in previous years the depth of the merged flow was less, about 5 Mm, and the common flow at that depth zero. This behaviour is clear in Method 1, and at least consistent with the results of Method 2.

No clear evidence for longitudinal structure emerges from the individual spectra. At most, we can say that at all locations there is a tendency for the meridional flow to progress from positive (northward) to negative (southward) values as depth increases. There is evidence of a meridional counter-cell at depth at the highest latitude in 2001 in Method 2, but this is not supported by Method 1.

The zonal flow departures from the standard differential rotation used to track exhibit no evident latitudinal dependence near the equator. This contrasts with the results for 2001 in particular, when there was a consistent latitudinal trend in the residuals, both at the surface and at depth.

ACKNOWLEDGMENTS

This work uses data from the Michelson Doppler Imager (MDI) on SOHO, a project of international cooperation between ESA and NASA. The MDI project is supported by NASA contract NAG5-13261 to Stanford University. This work was supported in part by NASA grants NAG5-10912 to SB and NAG5-11920 to DH.

REFERENCES

Basu S., Antia H. M. 1999. ApJ **525,** 517.

Haber D. A, Hindman B. W., Toomre J., Bogart R. S., Larsen R. M. Hill F. 2002. ApJ **570,** 855.

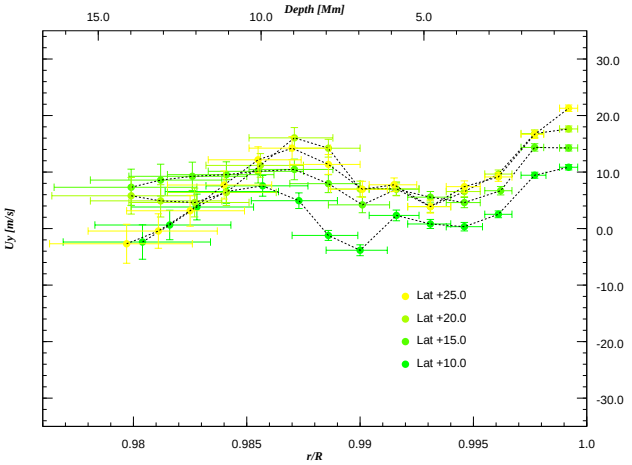

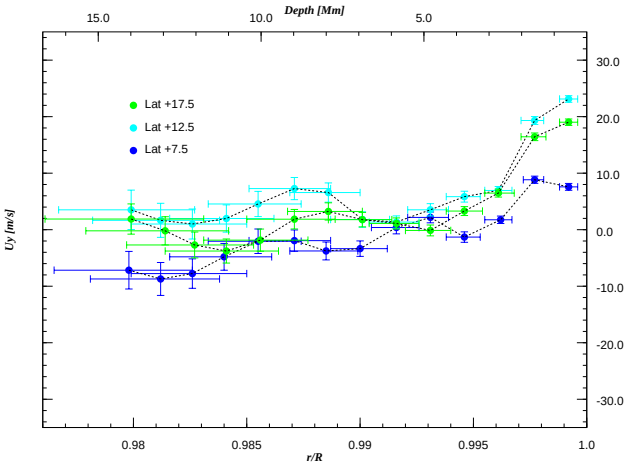

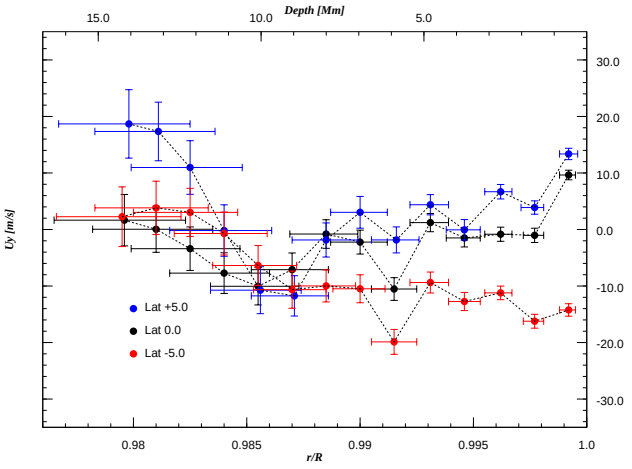

Figure 2. Inversions for meridional velocity a function of depth for the averages of power spectra for each tracked latitude using Method 1. Results for the three different campaigns are shown separately: (top) 1997; (middle) 2001; (bottom) 2004, with values for individual latitudes color coded.

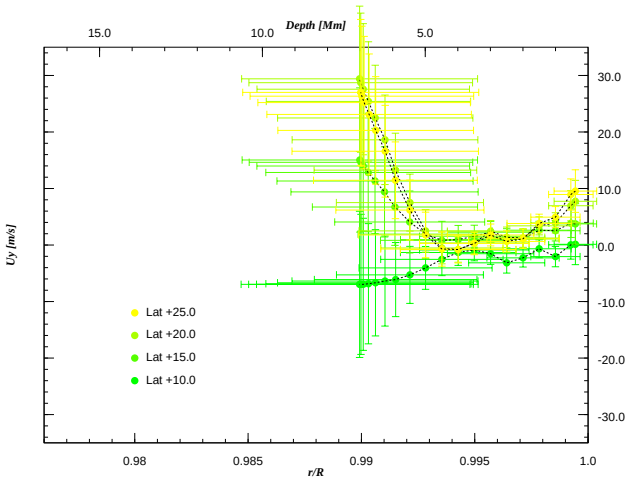

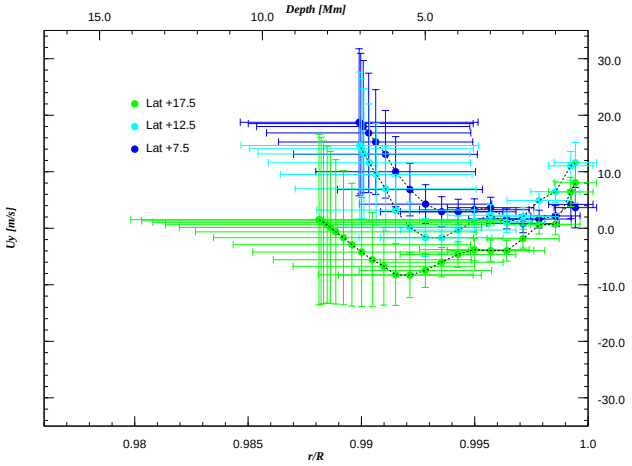

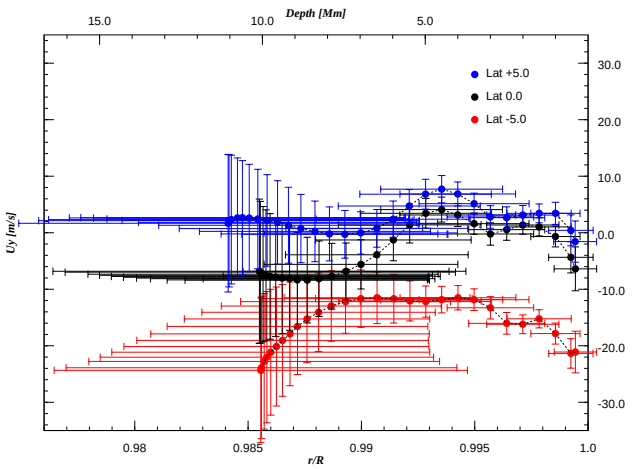

Figure 3. Same as Figure 2, but with inversions using Method 2.

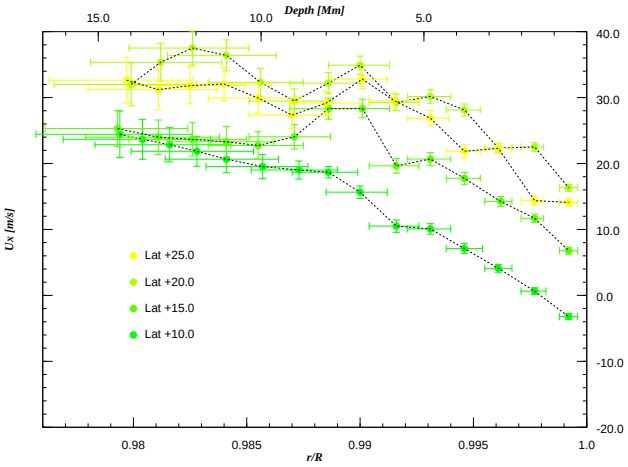

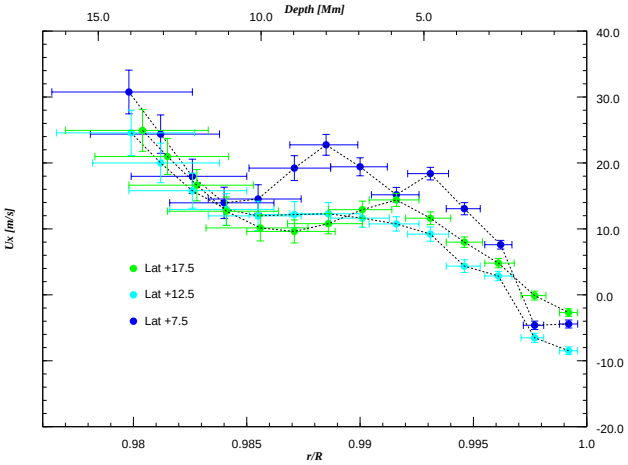

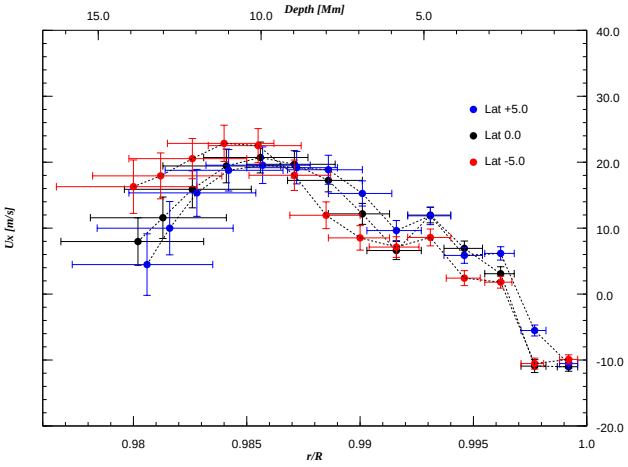

Figure 4. Same as Figure 2, but showing the inversions for zonal velocity.

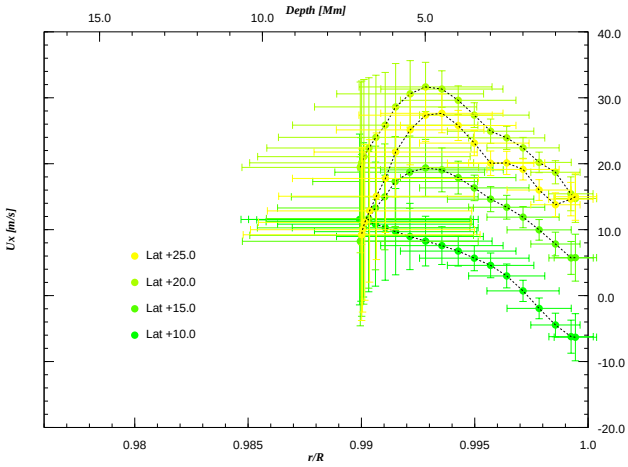

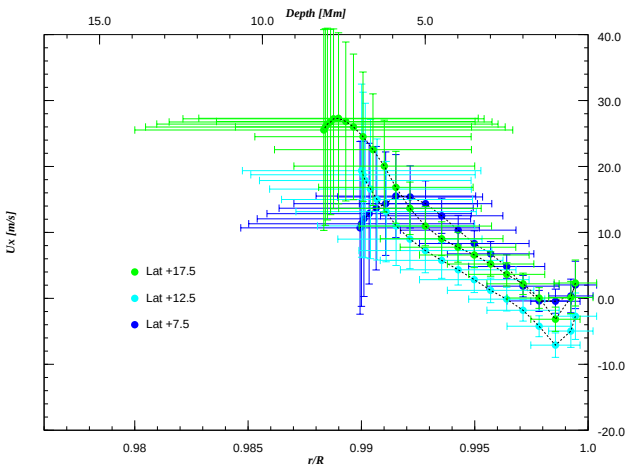

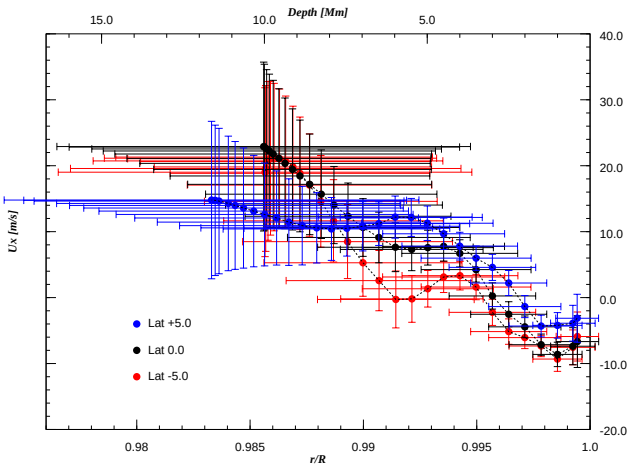

Figure 5. Same as Figure 4, but showing the inversions for zonal velocity.